PTEP

Prog. Theor. Exp. Phys. **2022** 12B105(17 pages)
DOI: 10.1093/ptep/ptac056

IYBSSD2022
International Year
of Basic Sciences
for Sustainable Development

Neutrino oscillation phenomenology and the impact of Professor Masatoshi Koshiba

Osamu Yasuda*

Department of Physics, Tokyo Metropolitan University, Hachioji, Tokyo 192-0397, Japan
*E-mail: yasuda@phys.se.tmu.ac.jp

Received February 2, 2022; Revised March 15, 2022; Accepted March 23, 2022; Published March 25, 2022

Neutrino oscillation phenomenology is briefly reviewed, and the impact of the late Professor Masatoshi Koshiba on research on the neutrino oscillation is discussed from the viewpoint of phenomenology.

Subject Index flavor mixing, neutrino mass, neutrino oscillation

1. Introduction

Since the announcement of the discovery of the atmospheric neutrino oscillation by the Super-Kamiokande Collaboration [1] in 1998, there has been remarkable progress in research on it. In this article I briefly describe neutrino oscillation phenomenology and I emphasize the impact of Professor Koshiba on neutrino oscillation study.

2. Three-flavor neutrino oscillation

2.1 *Preliminary*

If we assume a neutrino mass, we have to describe neutrinos in terms of the Dirac equation for spinors with masses. The mass eigenstates ν_j ($j = 1, 2, 3$) of neutrinos with mass m_j in vacuum can be described by the free Dirac equation. The Dirac equation of a spinor with mass m and momentum $\vec{p}$ has the energy eigenvalues $E, E, -E, -E$ where $E \equiv \sqrt{\vec{p}^2 + m^2}$. If we extract one component with the positive energy of ν_j, then the mass eigenstates ν_j ($j = 1, 2, 3$) of neutrinos satisfy the Dirac equation in vacuum:

$$i\frac{d}{dt}\nu_j(t) = E_j\,\nu_j(t), \quad E_j \equiv \sqrt{\vec{p}^2 + m_j^2}. \tag{1}$$

On the other hand, the flavor eigenstates of neutrinos $((\nu_e, \nu_\mu, \nu_\tau)^T)$ are those that can be observed in the processes $\nu_e + n \to e^- + p$, $\nu_\mu + n \to \mu^- + p$, $\nu_\tau + n \to \tau^- + p$. The mass $((\nu_1, \nu_2, \nu_3)^T)$ and flavor $((\nu_e, \nu_\mu, \nu_\tau)^T)$ eigenstates of the neutrino sector are related by

$$\begin{pmatrix} \nu_e \\ \nu_\mu \\ \nu_\tau \end{pmatrix} = U \begin{pmatrix} \nu_1 \\ \nu_2 \\ \nu_3 \end{pmatrix},$$

Funded by SCOAP³. SCOAP3 and OUP support the goals of the International Year of Basic Sciences for Sustainable Development

where

$$U \equiv \begin{pmatrix} 1 & 0 & 0 \\ 0 & c_{23} & s_{23} \\ 0 & -s_{23} & c_{23} \end{pmatrix} \begin{pmatrix} c_{13} & 0 & s_{13}e^{-i\delta} \\ 0 & 1 & 0 \\ -s_{13}e^{i\delta} & 0 & c_{13} \end{pmatrix} \begin{pmatrix} c_{12} & s_{12} & 0 \\ -s_{12} & c_{12} & 0 \\ 0 & 0 & 1 \end{pmatrix}$$
$$= \begin{pmatrix} c_{12}c_{13} & s_{12}c_{13} & s_{13}e^{-i\delta} \\ -s_{12}c_{23} - c_{12}s_{23}s_{13}e^{i\delta} & c_{12}c_{23} - s_{12}s_{23}s_{13}e^{i\delta} & s_{23}c_{13} \\ s_{12}s_{23} - c_{12}c_{23}s_{13}e^{i\delta} & -c_{12}s_{23} - s_{12}c_{23}s_{13}e^{i\delta} & c_{23}c_{13} \end{pmatrix} \tag{2}$$

is the 3×3 unitary neutrino mixing matrix [2,3], $\theta_{12}, \theta_{23}, \theta_{13}$ are three mixing angles, δ is a CP phase, and $c_{jk} \equiv \cos\theta_{jk}$, $s_{jk} \equiv \sin\theta_{jk}$. It is known that the propagation of neutrinos in matter is described with the matter effect [4,5]:

$$i\frac{d}{dt}\begin{pmatrix} \nu_e(t) \\ \nu_\mu(t) \\ \nu_\tau(t) \end{pmatrix} = M \begin{pmatrix} \nu_e(t) \\ \nu_\mu(t) \\ \nu_\tau(t) \end{pmatrix} \tag{3}$$

$$M \equiv [U\,\mathrm{diag}(E_1, E_2, E_3)\,U^{-1} + \mathrm{diag}(A_{\mathrm{CC}} + A_{\mathrm{NC}}, A_{\mathrm{NC}}, A_{\mathrm{NC}})]$$
$$= [U\,\mathrm{diag}(0, \Delta E_{21}, \Delta E_{31})\,U^{-1} + \mathrm{diag}(A_{\mathrm{CC}}, 0, 0) + (E_1 + A_{\mathrm{NC}})\,\mathbf{1}], \tag{4}$$

where $\Delta E_{jk} \equiv E_j - E_k \simeq (m_j^2 - m_k^2)/2|\vec{p}| \equiv \Delta m_{jk}^2/2|\vec{p}| \simeq \Delta m_{jk}^2/2E$,

$$A_{\mathrm{CC}} \equiv \sqrt{2}\,G_F N_e = \left[\frac{\rho}{2.6\ (\mathrm{g\cdot cm^{-3}})}\right] \cdot \left(\frac{Y_e}{0.5}\right) \cdot 1.0 \times 10^{-13}\,\mathrm{eV}$$

$$A_{\mathrm{NC}} \equiv -\frac{1}{\sqrt{2}}\,G_F N_n = -\left[\frac{\rho}{2.6\ (\mathrm{g\cdot cm^{-3}})}\right] \cdot \left(\frac{1 - Y_e}{0.5}\right) \cdot 5.0 \times 10^{-14}\,\mathrm{eV}$$

stand for the matter effect due to the charged and neutral current interactions, N_e and N_n stand for the density of electrons and neutrons, $G_F = 1.166 \times 10^{-5}\ \mathrm{GeV}^{-2}$ is the Fermi coupling constant, and $Y_e = N_p/(N_p + N_n)$ is the relative number density of electrons in matter, where N_p represents the number of protons per unit volume. Since the term that is proportional to the 3×3 identity matrix $\mathbf{1}$ only affects the overall phase of the probability amplitude $A(\nu_\alpha \to \nu_\beta)$, $(E_1 + A_{\mathrm{NC}})\,\mathbf{1}$ in Eq. (4) can be ignored.

2.2 *Mixing angles and mass-squared differences*

If the density is constant, then Eq. (4) can be formally diagonalized as

$$M = \tilde{U}\,\mathrm{diag}(\tilde{E}_1, \tilde{E}_2, \tilde{E}_3)\,\tilde{U}^{-1},$$

where $\tilde{E}_j$ $(j = 1, 2, 3)$ are the energy eigenvalues of M in matter, and $\tilde{U}$ is a unitary matrix that diagonalizes M. The probability $P(\nu_\alpha \to \nu_\beta)$ can be expressed as

$$P(\nu_\alpha \to \nu_\beta) = \delta_{\alpha\beta} - 4\sum_{j<k} \mathrm{Re}\big(\tilde{U}_{\alpha j}\tilde{U}_{\beta j}^*\tilde{U}_{\alpha k}^*\tilde{U}_{\beta k}\big)\sin^2\left(\frac{\Delta\tilde{E}_{jk}L}{2}\right)$$
$$- 2\sum_{j<k} \mathrm{Im}\big(\tilde{U}_{\alpha j}\tilde{U}_{\beta j}^*\tilde{U}_{\alpha k}^*\tilde{U}_{\beta k}\big)\sin(\Delta\tilde{E}_{jk}L), \tag{5}$$

where $\Delta\tilde{E}_{jk} \equiv \tilde{E}_j - \tilde{E}_k$.

From the parametrization (2), the simplest mixing angle to determine is θ_{13}. If we consider the disappearance experiment of reactor neutrinos with a baseline length $L = 2$ km, where the mean neutrino energy is $E \simeq 4$ MeV, and if we assume that the contribution from the smaller mass-squared difference $\Delta m_{21}^2 L/2E$ is small, then, because the matter effect, which appears in

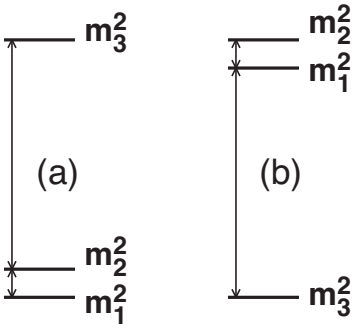

Fig. 1. Two mass patterns: (a) normal ordering ($\Delta m^2_{31} > 0$), (b) inverted ordering ($\Delta m^2_{31} < 0$). Both mass patterns are allowed as of 2021.

the form of $A_{\rm CC}L/2 \sim L/(4000\ {\rm km})$ in the oscillation probability, can be ignored, we obtain

$$P(\bar{\nu}_e \to \bar{\nu}_e) \simeq 1 - 4|U_{e3}|^2(1-|U_{e3}|^2)\sin^2\left(\frac{\Delta m^2_{31}L}{4E}\right)$$
$$= 1 - \sin^2 2\theta_{13}\sin^2\left(\frac{\Delta m^2_{31}L}{4E}\right). \tag{6}$$

Equation (6) has the same form as the oscillation probability in the two-flavor framework, and one can get information on θ_{13} from the result that is expressed in terms of the two-flavor oscillation analysis. From the negative result of the Chooz reactor neutrino experiment [6], we obtain

$$\sin^2 2\theta_{13} \lesssim 0.15 \quad \text{for } |\Delta m^2_{31}| = 2.5\times 10^{-3}{\rm eV}^2\ (90\%\ {\rm CL}). \tag{7}$$

Equation (7) shows that θ_{13} is small, so we can put $\theta_{13} \to 0$ in the zeroth approximation. If we consider the case where $|\Delta E_{21}| \simeq |\Delta m^2_{21}/2E| \ll |\Delta E_{31}| \simeq |\Delta m^2_{31}/2E| \sim A_{\rm CC}$, then the term that is proportional to ΔE_{21} in Eq. (4) can be ignored, so θ_{12} as well as θ_{13} disappear, the ν_e state decouples from the ν_μ and ν_τ states (i.e., the matter effect disappears from the sector of ν_μ and ν_τ), and we get

$$P(\nu_\mu \to \nu_\mu) \simeq 1 - 4|U_{\mu 3}|^2(1-|U_{\mu 3}|^2)\sin^2\left(\frac{\Delta m^2_{31}L}{4E}\right)$$
$$\simeq 1 - \sin^2 2\theta_{23}\sin^2\left(\frac{\Delta m^2_{31}L}{4E}\right). \tag{8}$$

Again Eq. (8) has the same form as the oscillation probability in the two-flavor framework. From the results of atmospheric neutrino measurements of the Super-Kamiokande experiment [1], we have

$$\sin^2\theta_{23} \simeq 0.5 \tag{9}$$

$$\left|\Delta m^2_{31}\right| \simeq 2.5\times 10^{-3}\,{\rm eV}^2. \tag{10}$$

Notice that the sign of Δm^2_{31} cannot be determined from Eq. (8) because it is invariant under the change of the sign of Δm^2_{31}. The mass pattern for $\Delta m^2_{31} > 0$ ($\Delta m^2_{31} < 0$) is called normal (inverted) ordering, and is depicted in Fig. 1.

As for (θ_{12}, Δm^2_{21}), there are two ways to determine them. The first one is from KamLAND [7], the long baseline reactor experiment. If we put $\theta_{13} \to 0$ again, then in the zeroth approximation we have $A_{\rm CC} \ll |\Delta E_{21}| \simeq |\Delta m^2_{21}/2E| \ll |\Delta E_{31}| \simeq |\Delta m^2_{31}/2E|$, because the matter effect,

which appears in the form of $A_{\rm CC}L \sim L/(2000\ {\rm km})$ in the oscillation probability, can be ignored. Hence we obtain the oscillation probability

$$P(\bar{\nu}_e \to \bar{\nu}_e) \simeq 1 - 4|U_{e1}|^2|U_{e2}|^2 \sin^2\left(\frac{\Delta m^2_{21}L}{4E}\right)$$
$$\simeq 1 - \sin^2 2\theta_{12} \sin^2\left(\frac{\Delta m^2_{21}L}{4E}\right), \tag{11}$$

which has the same form as the oscillation probability in the two-flavor framework. From the KamLAND result, we get

$$\sin^2\theta_{12} \simeq 0.3 \tag{12}$$

$$\left|\Delta m^2_{21}\right| \simeq 8 \times 10^{-5}\ {\rm eV}^2. \tag{13}$$

The other way to determine $(\theta_{12}, \Delta m^2_{21})$ is from solar neutrino observations. In the case of solar neutrinos, we have to take into account the fact that the density of electrons varies (we know now that it varies adiabatically) from the production point of neutrinos near the center of the Sun all the way to the Earth. If we assume that the electron density varies adiabatically, then the oscillation probability $P(\nu_e \to \nu_e)$ is given by

$$P\left(\nu_e \to \nu_e\right) = \sum_{j,k} \tilde{U}_{ej}(L)\tilde{U}^*_{ek}(L)\tilde{U}^*_{ej}(0)\tilde{U}_{ek}(0) \exp\left(-i\int_0^L dt\ \Delta\tilde{E}_{jk}\right), \tag{14}$$

where $t = 0$ ($t = L$) stands for the production (detection) point, and we discuss here the detection of solar neutrinos during the day; i.e., the density at the detection point is approximately zero. Since the distance L between the Sun and the Earth is literally astronomically large, we have $|\int_0^L dt\ \Delta\tilde{E}_{jk}| \gg 1$ $(j \neq k)$, so by averaging over rapid oscillations, we can put $\exp(-i\int_0^L dt\ \Delta\tilde{E}_{jk}) \to \delta_{jk}$. Thus we get

$$P(\nu_e \to \nu_e) = \sum_j \tilde{U}_{ej}(L)\tilde{U}^*_{ej}(L)\tilde{U}^*_{ej}(0)\tilde{U}_{ej}(0)$$
$$= \sum_j |U_{ej}|^2|\tilde{U}_{ej}(0)|^2, \tag{15}$$

where the mixing matrix $\tilde{U}(L)$ at the detection point $t = L$ was replaced by the one U in vacuum because the density there is assumed to be zero. If take the limit $\theta_{13} \to 0$, then Eq. (15) reduces to the two-flavor case. In the two-flavor case, the effective mixing angle is given by

$$\cos 2\tilde{\theta}_{12} \equiv \frac{1}{\Delta\tilde{E}_{21}}(\Delta E_{21}\cos 2\theta_{12} - A_{\rm CC}),$$
$$\Delta\tilde{E}_{21} \equiv \{[\Delta E_{21}\cos 2\theta_{12} - A_{\rm CC})]^2 + (\Delta E_{21}\sin 2\theta_{12})^2\}^{1/2}.$$

Since the effective mixing matrix elements in the two-flavor case are given by $|\tilde{U}_{e1}(0)|^2 = \cos^2\tilde{\theta}_{12}$ and $|\tilde{U}_{e2}(0)|^2 = \sin^2\tilde{\theta}_{12}$, we have

$$P(\nu_e \to \nu_e) \simeq \frac{1}{2}\left(1 + \cos 2\theta_{12}\frac{\Delta E_{21}\cos 2\theta_{12} - A_{\rm CC}(0)}{\Delta\tilde{E}_{21}(0)}\right), \tag{16}$$

where the argument (0) stands for the quantity evaluated at the production point of neutrinos. From the oscillation probability (16) and the data of various experiments that measure $P(\nu_e \to \nu_e)$ at different solar neutrino energies, the following results are obtained [8]:

$$\sin^2\theta_{12} \simeq 0.3 \tag{17}$$

$$\Delta m^2_{21} \simeq 6 \times 10^{-5}\,\mathrm{eV}^2, \tag{18}$$

which are approximately consistent with the results (12) and (13) from KamLAND. Notice that the result from solar neutrino measurements is able to determine the sign of Δm^2_{21} because of the matter effect, while KamLAND gives little information on the sign of Δm^2_{21} since the oscillation probability (11) for KamLAND is basically that in vacuum and therefore it is invariant under the change of the sign of Δm^2_{21}.

2.3 *Parameter degeneracy*

To determine the CP phase δ, precise measurements of the oscillation probabilities are required, since the effect of δ appears only in the combination of $s_{13}e^{\pm i\delta}$ as we can see from Eq. (2). It is expected that long baseline accelerator-based experiments are advantageous to perform precise measurements, because one can control the baseline length and the neutrino energy. Conventional neutrino beams, which can be obtained from pion decays, are ν_μ and $\bar{\nu}_\mu$, so $\nu_\mu \to \nu_e$ and $\bar{\nu}_\mu \to \bar{\nu}_e$ are the two major channels to determine the CP phase. Now the question is, given the appearance probabilities $P(\nu_\mu \to \nu_e) = \text{constant} \equiv P$ and $P(\bar{\nu}_\mu \to \bar{\nu}_e) = \text{constant} \equiv \bar{P}$ in addition to the disappearance probabilities $P(\nu_\mu \to \nu_\mu) = \text{constant}$ and $P(\bar{\nu}_\mu \to \bar{\nu}_\nu) = \text{constant}$, is it possible to determine δ uniquely? The answer to this question turns out to be negative because there are eight possible values for δ, and this is called eightfold parameter degeneracy. In the approximation to second order in θ_{13} and Δm^2_{21}, the appearance probabilities can be written as [9,10]

$$P(\nu_\mu \to \nu_e) = x^2F^2 + 2\,\mathrm{sign}\left(\Delta m^2_{31}\right) xyFg\cos\left[\delta + \mathrm{sign}\left(\Delta m^2_{31}\right)\Delta\right] + y^2g^2 = P \tag{19}$$

$$P(\bar{\nu}_\mu \to \bar{\nu}_e) = x^2\bar{F}^2 + 2\,\mathrm{sign}\left(\Delta m^2_{31}\right) xy\bar{F}g\cos\left[\delta - \mathrm{sign}\left(\Delta m^2_{31}\right)\Delta\right] + y^2g^2 = \bar{P}, \tag{20}$$

where

$$\begin{aligned}
x &\equiv s_{23}\sin 2\theta_{13} \\
y &\equiv \alpha c_{23}\sin 2\theta_{12} \\
(F, \bar{F}) &\equiv \begin{cases} (f, \bar{f}) & \text{for NO} \\ (\bar{f}, f) & \text{for IO} \end{cases} \\
\begin{Bmatrix} f \\ \bar{f} \end{Bmatrix} &\equiv \frac{\sin(\Delta \mp A_{\mathrm{CC}}L/2)}{(1 \mp A_{\mathrm{CC}}L/2\Delta)}, \\
g &\equiv \frac{\sin(A_{\mathrm{CC}}L/2)}{A_{\mathrm{CC}}L/2\Delta} \\
\Delta &\equiv \frac{|\Delta m^2_{31}|L}{4E} = 1.27 \times \frac{\left(|\Delta m^2_{31}|/\mathrm{eV}^2\right)(L/\mathrm{km})}{(E/\mathrm{GeV})} \\
\alpha &\equiv \left|\frac{\Delta m^2_{21}}{\Delta m^2_{31}}\right|.
\end{aligned} \tag{21}$$

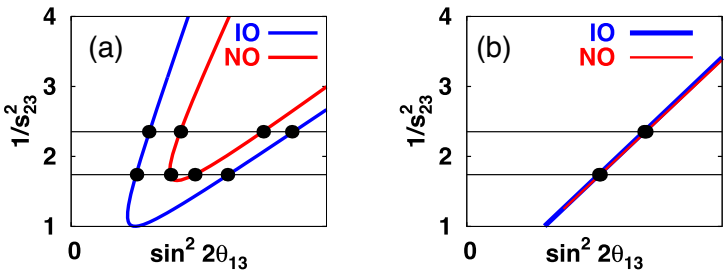

Fig. 2. Parameter degeneracy for normal ordering (NO) and inverted ordering (IO): (a) off the oscillation maximum ($|\Delta m^2_{31}|L/4E \neq \pi/2$), (b) at the oscillation maximum ($|\Delta m^2_{31}|L/4E = \pi/2$). In the case of (a), there are eight solutions with different values of δ. In the case of (b), there are four solutions with twofold degeneracy.

Defining $X \equiv \sin^2 2\theta_{13}$, $Y \equiv 1/s^2_{23}$, and eliminating δ, we obtain the following expression from Eqs. (19) and (20) [11]:

$$16CX(Y-1) = \frac{1}{\cos^2\Delta}\left[\left(\frac{P-C}{F}+\frac{\bar{P}-C}{\bar{F}}\right)(Y-1)-(F+\bar{F})X+\frac{P}{F}+\frac{\bar{P}}{\bar{F}}\right]^2 + \frac{1}{\sin^2\Delta}\left[\left(\frac{P-C}{F}-\frac{\bar{P}-C}{\bar{F}}\right)(Y-1)-(F-\bar{F})X+\frac{P}{F}-\frac{\bar{P}}{\bar{F}}\right]^2, \quad (22)$$

where

$$C \equiv \left(\frac{\Delta m^2_{21}}{\Delta m^2_{31}}\right)^2\left[\frac{\sin(A_{\rm CC}L/2)}{A_{\rm CC}L/2\Delta}\right]^2 \sin^2 2\theta_{12}.$$

Equation (22) gives a quadratic curve in the (X, Y)-plane. At the oscillation maximum ($|\Delta m^2_{31}|L/4E = \pi/2$), the numerator of the first term on the right-hand side of Eq. (22) must vanish, and it yields a straight line in the (X, Y)-plane:

$$\left(\frac{P-C}{F}+\frac{\bar{P}-C}{\bar{F}}\right)(Y-1)-(F+\bar{F})X+\frac{P}{F}+\frac{\bar{P}}{\bar{F}}=0. \quad (23)$$

Equations (22) and (23) are depicted in Figs. 2(a) and (b).

As can be seen from Fig. 2, there are eight (four) solutions in general off (at) the oscillation maximum. This parameter degeneracy is in general eightfold [10], since there are two intersections between the curve (22) and $Y =$ constant due to the quadratic nature of the curve (22) (intrinsic degeneracy [12]), there are two curves depending on whether the mass ordering is normal (red in Fig. 2) or inverted (blue) (sign degeneracy [13]), and there are two possibilities for the θ_{23} octant given a value of $\sin^2 2\theta_{23}$ (octant degeneracy [14]). The problem with this parameter degeneracy is that the value of δ is different for a different point in Fig. 2, and we must resolve this degeneracy to determine δ precisely. In particular, it is known [10] that the value of δ depends strongly on the mass ordering, so even if the long baseline experiment is done at the oscillation maximum, the resolution of sign degeneracy is important to determine δ.

2.4 *Status of measurements of the oscillation parameters*

Measurements of θ_{13} have been done by the appearance channel $\nu_\mu \to \nu_e$ at the accelerator neutrino experiments, T2K [15], MINOS [16], and by the disappearance channel $\bar{\nu}_e \to \bar{\nu}_e$ at the reactor neutrino experiments, Double Chooz [17], Daya Bay [18], and Reno [19], and θ_{13} has been determined precisely. On the other hand, the two long baseline experiments, T2K [20] and

Table 1. The updated results of the global fit by the three groups. The definition of the mass-squared difference $\Delta m^2_{\rm atm}$ of atmospheric neutrino oscillation is different for different groups. Although two different results, with and without the Super-Kamiokande atmospheric neutrino data, are presented in Ref. [22], only those with the atmospheric neutrino data are quoted. Normal ordering gives the best fit, but the significance of NO over IO is not strong enough to exclude IO yet.

Ref.	[22] w SK-ATM		[23] w SK-ATM		[24] w SK-ATM	
Date of update	29 Nov 2021		28 Sep 2021		19 Jan 2021	
NO	Best-fit ordering		Best-fit ordering		Best-fit ordering	
Param	bfp $\pm 1\sigma$	3σ range	bfp $\pm 1\sigma$	3σ range	bfp $\pm 1\sigma$	3σ range
$\sin^2\theta_{12}/10^{-1}$	$3.04^{+0.12}_{-0.12}$	$2.69 \to 3.43$	$3.03^{+0.13}_{-0.13}$	$2.63 \to 3.45$	$3.18^{+0.16}_{-0.16}$	$2.71 \to 3.69$
$\theta_{12}/^\circ$	$33.5^{+0.8}_{-0.8}$	$31.3 \to 35.9$	$33.4^{+0.8}_{-0.8}$	$30.9 \to 36.0$	$34.3^{+1.0}_{-1.0}$	$31.4 \to 37.4$
$\sin^2\theta_{23}/10^{-1}$	$4.50^{+0.19}_{-0.16}$	$4.08 \to 6.03$	$4.55^{+0.18}_{-0.15}$	$4.16 \to 5.99$	$5.74^{+0.14}_{-0.14}$	$4.34 \to 6.10$
$\theta_{23}/^\circ$	$42.1^{+1.1}_{-0.9}$	$39.7 \to 50.9$	$42.4^{+1.0}_{-0.9}$	$40.2 \to 50.7$	$49.3^{+0.8}_{-0.8}$	$41.2 \to 51.3$
$\sin^2\theta_{13}/10^{-2}$	$2.25^{+0.06}_{-0.06}$	$2.06 \to 2.44$	$2.23^{+0.07}_{-0.06}$	$2.04 \to 2.44$	$2.20^{+0.07}_{-0.06}$	$2.00 \to 2.41$
$\theta_{13}/^\circ$	$8.62^{+0.12}_{-0.12}$	$8.25 \to 8.98$	$8.59^{+0.13}_{-0.12}$	$8.21 \to 8.99$	$8.53^{+0.13}_{-0.12}$	$8.13 \to 8.92$
$\delta/^\circ$	230^{+36}_{-25}	$144 \to 350$	274^{+25}_{-27}	$139 \to 355$	194^{+24}_{-22}	$128 \to 359$
$\Delta m^2_{21}/10^{-5}$ eV^2	$7.42^{+0.21}_{-0.20}$	$6.82 \to 8.04$	$7.36^{+0.16}_{-0.15}$	$6.93 \to 7.93$	$7.50^{+0.22}_{-0.20}$	$6.94 \to 8.14$
$\Delta m^2_{\rm atm}/10^{-3}$ eV^2	$2.51^{+0.03}_{-0.03}$	$2.43 \to 2.59$	$2.49^{+0.02}_{-0.03}$	$2.40 \to 2.57$	$2.55^{+0.02}_{-0.03}$	$2.47 \to 2.63$
IO	$\Delta\chi^2 = 7.0$		$\Delta\chi^2 = 6.5$		$\Delta\chi^2 = 6.4$	
$\sin^2\theta_{12}/10^{-1}$	$3.04^{+0.13}_{-0.12}$	$2.69 \to 3.43$	$3.03^{+0.13}_{-0.13}$	$2.63 \to 3.45$	$3.18^{+0.16}_{-0.16}$	$2.71 \to 3.69$
$\theta_{12}/^\circ$	$33.5^{+0.8}_{-0.8}$	$31.3 \to 35.9$	$33.4^{+0.8}_{-0.8}$	$30.9 \to 36.0$	$34.3^{+1.0}_{-1.0}$	$31.4 \to 37.4$
$\sin^2\theta_{23}/10^{-1}$	$5.70^{+0.16}_{-0.22}$	$4.10 \to 6.13$	$5.69^{+0.13}_{-0.21}$	$4.17 \to 6.06$	$5.78^{+0.10}_{-0.17}$	$4.33 \to 6.08$
$\theta_{23}/^\circ$	$49.0^{+0.9}_{-1.3}$	$39.8 \to 51.6$	$49.0^{+0.8}_{-1.2}$	$40.22 \to 51.12$	$49.5^{+0.6}_{-1.0}$	$41.2 \to 51.3$
$\sin^2\theta_{13}/10^{-2}$	$2.24^{+0.07}_{-0.06}$	$2.06 \to 2.46$	$2.23^{+0.06}_{-0.06}$	$2.03 \to 2.45$	$2.23^{+0.06}_{-0.07}$	$2.02 \to 2.42$
$\theta_{13}/^\circ$	$8.61^{+0.14}_{-0.12}$	$8.24 \to 9.02$	$8.59^{+0.12}_{-0.12}$	$8.19 \to 9.01$	$8.58^{+0.12}_{-0.14}$	$8.17 \to 8.96$
$\delta/^\circ$	278^{+22}_{-30}	$194 \to 345$	274^{+25}_{-27}	$193 \to 342$	284^{+26}_{-28}	$200 \to 353$
$\Delta m^2_{21}/10^{-5}$ eV^2	$7.42^{+0.21}_{-0.20}$	$6.82 \to 8.04$	$7.36^{+0.16}_{-0.15}$	$6.93 \to 7.93$	$7.50^{+0.22}_{-0.20}$	$6.94 \to 8.14$
$\Delta m^2_{\rm atm}/10^{-3}$ eV^2	$2.49^{+0.03}_{-0.03}$	$2.41 \to 2.57$	$2.46^{+0.03}_{-0.03}$	$2.38 \to 2.54$	$2.45^{+0.02}_{-0.03}$	$2.37 \to 2.53$
Def of $\Delta m^2_{\rm atm}$	$\max\left(\lvert\Delta m^2_{31}\rvert, \lvert\Delta m^2_{32}\rvert\right)$		$\lvert m^2_3 - (m^2_1 + m^2_2)/2\rvert$		$\lvert\Delta m^2_{31}\rvert$	

NOvA [21], are performed approximately at the oscillation maximum, so the present situation is approximately described by Fig. 2(b).

Table 1 gives the results by the three groups [22–24] for the values of the mixing angles and the mass-squared differences from global analysis of solar neutrinos (Chlorine [25], GALLEX/GNO [26], SAGE [27], and Super-Kamiokande [8,28–30], SNO [31], and Borexino [32–34]), KamLAND [35], atmospheric neutrinos (Super-Kamiokande [36] and IceCube/DeepCore [37,38]) medium baseline reactor neutrinos (Double Chooz [39], Daya Bay [40], and RENO [41]), the disappearance channel at accelerator-based long baseline experiments (MINOS [42], T2K [43], and NOvA [44]), and the appearance channel at accelerator-based long baseline experiments (MINOS [45], T2K [43], and NOvA [44]). As can be seen from Eq. (21), the matter effect appears in the form $A_{\rm CC}L/2 \sim L/4000$ km. Since the baseline lengths of T2K and NOvA are not long enough to satisfy $A_{\rm CC}L/2 \sim O(1)$, the results by these long baseline experiments are not conclusive enough to determine the mass pattern as of 2021. Octant degeneracy is also unresolved.

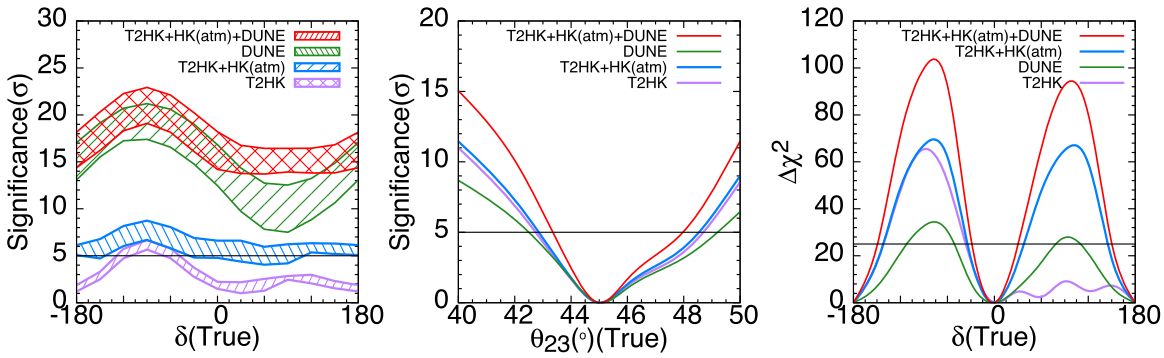

Fig. 3. Sensitivity of the future experiments and their combinations to the unknown quantities in the case of normal ordering [49]. Left: Significance of mass ordering as a function of the true value of the CP phase δ. Middle: Significance of the octant as a function of the true value of θ_{23}. Right: $\Delta\chi^2 = \{\text{significanceofCPviolation}(\sigma)\}^2$ as a function of the true value of the CP phase δ. The horizontal straight line in each panel stands for 5σ, which corresponds to discovery.

2.5 *Prospects in future experiments*

The quantities that are not determined as of 2021 are the pattern of mass ordering (the two mass patterns in Fig. 1 are allowed at present), the octant of θ_{23} (in other words the sign of $(\theta_{23} - 45^\circ)$), and the CP phase δ. Determination of the mass ordering, the octant of θ_{23}, and the CP phase δ is expected to be carried out in future long baseline experiments, T2HK [46] and DUNE [47]. Figure 3 shows the sensitivity of these experiments together with atmospheric neutrino measurements at the Hyper-Kamiokande (HK) experiment [48] to the unknown quantities. The DUNE experiment has a baseline length $L = 1300$ km, and it has the highest sensitivity to the mass ordering and the significance to reject wrong mass ordering is at least 7σ for any value of δ. T2HK has a short baseline length $L = 295$ km, and it has therefore poor sensitivity to the mass ordering, but if it is combined with the HK atmospheric neutrino data, then the significance to reject wrong mass ordering is at least 4σ. Octant degeneracy is expected to be solved if $|\theta_{23} - 45^\circ| > 3^\circ$ if we combine T2HK, DUNE, and HK atmospheric neutrinos. As for the CP phase, unless δ is close to 0 or 180°, DUNE, the combination of T2HK and atmospheric neutrino observation at HK, and the combination of all these can exclude the hypothesis that $\delta = 0$ or $\delta = 180^\circ$.

3. New physics beyond the Standard Model with three massive neutrinos

As of 2021, there are several anomalies that cannot be accounted for by the standard three-flavor framework. One is a class of anomalies that may be explained if we assume the existence of light sterile neutrinos [50] whose mass is of order 1 eV. They are the results of LSND [51], MiniBooNE [52], the reactor antineutrino anomaly [53,54], and the gallium anomaly [55]. Also, the recent IceCube data [56] suggests a mild preference for light sterile neutrinos in the disappearance channel $\nu_\mu \to \nu_\mu + \bar{\nu}_\mu \to \bar{\nu}_\mu$. The other anomaly is the discrepancy [57] between the mass-squared differences of the solar and KamLAND experiments. This may be explained [58,59] if we assume either flavor-dependent non-standard interactions during the propagation of neutrinos [4,60,61], or light sterile neutrinos whose mass-squared difference is of order 10^{-5} eV^2. These anomalies have attracted a lot of attention because they may provide us a key to physics beyond the Standard Model.

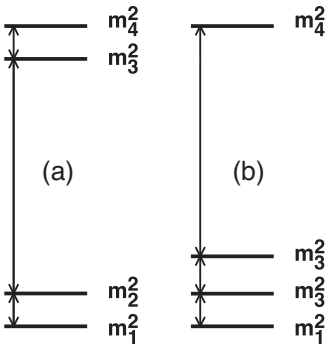

Fig. 4. Two schemes of four-neutrino mixing. (a) (2+2)-scheme, (b) (3+1)-scheme.

3.1 *Light sterile neutrinos*

If we assume four flavor and mass eigenstates, then the fourth flavor eigenstate must be a sterile neutrino state ν_s, which is singlet with respect to the gauge group of the Standard Model because the number of weakly interacting light neutrinos is three from the LEP data [62]. So the equation of motion is described by the following 4×4 Hamiltonian:

$$i\frac{d}{dt}\begin{pmatrix}\nu_e(t)\\ \nu_\mu(t)\\ \nu_\tau(t)\\ \nu_s(t)\end{pmatrix} = M\begin{pmatrix}\nu_e(t)\\ \nu_\mu(t)\\ \nu_\tau(t)\\ \nu_s(t)\end{pmatrix} \tag{24}$$

$$\begin{aligned} M &\equiv [U\,\mathrm{diag}(E_1, E_2, E_3, E_4)\,U^{-1} + \mathrm{diag}(A_{\mathrm{CC}}, 0, 0, -A_{\mathrm{NC}}) + A_{\mathrm{NC}}\,\mathbf{1}] \\ &= [U\,\mathrm{diag}(0, \Delta E_{21}, \Delta E_{31}, \Delta E_{41})\,U^{-1} + \mathrm{diag}(A_{\mathrm{CC}}, 0, 0, -A_{\mathrm{NC}}) + (E_1 + A_{\mathrm{NC}})\,\mathbf{1}]. \end{aligned} \tag{25}$$

The 4×4 mixing matrix U has six mixing angles and three CP phases, and one of the parametrizations for U is given by

$$U = R_{34}(\theta_{34}, \delta_{34})\; R_{24}(\theta_{24}, 0)\; R_{14}(\theta_{14}, \delta_{14})\; R_{23}(\theta_{23}, 0)\; R_{13}(\theta_{13}, \delta_{13})\; R_{12}(\theta_{12}, 0), \tag{26}$$

where $R_{ij}(\theta_{ij}, \delta_l)$ are complex rotation matrices in the ij-plane defined as:

$$[R_{ij}(\theta_{ij},\ \delta_{ij})]_{pq} = \begin{cases} \cos\theta_{ij} & p = q = i, j \\ 1 & p = q \neq i, j \\ \sin\theta_{ij}\, e^{-i\delta_{ij}} & p = i;\ q = j \\ -\sin\theta_{ij}\, e^{i\delta_{ij}} & p = j;\ q = i \\ 0 & \text{otherwise.} \end{cases}$$

The angles θ_{14}, θ_{24}, θ_{34} stand for the mixing of oscillations at short baseline experiments of reactor neutrino ($\bar{\nu}_e \to \bar{\nu}_e$) and radioactive sources ($\nu_e \to \nu_e$), that of oscillations at short baseline accelerator neutrino experiments ($\nu_\mu \to \nu_\mu$ and $\bar{\nu}_\mu \to \bar{\nu}_\mu$), and the ratio between $\nu_\mu \to \nu_\tau$ and $\nu_\mu \to \nu_s$ at short baseline accelerator neutrino experiments, respectively. In the limit $\theta_{j4} \to 0$ ($j = 1, 2, 3$), the mixing is reduced to the PMNS paradigm with $\delta = \delta_{13}$. In the case of four-neutrino mixing scenarios, there are two schemes, the (2+2)-scheme (Fig. 4(a)) and the (3+1)-scheme (Fig. 4(b)). The (2+2)-scheme is excluded by combining the constraints from the solar and atmospheric neutrinos [63]. On the other hand, in the (3+1)-scheme, three massive states must be on the lower side as in Fig. 2(b) because the one with three massive states on the upper side is excluded by the cosmological bound [62] $\sum_j m_j \lesssim 0.5$ eV (95% CL).

If the neutrino energy E and the baseline length L satisfy $|\Delta m^2_{41} L/E| \sim O(1)$ for the value $\Delta m^2_{41} \gtrsim 0.1\ \mathrm{eV}^2$, then the contributions from the smaller mass-squared differences Δm^2_{31} and Δm^2_{21} become negligible, and the oscillation probability in vacuum can be expressed as

$$P(\nu_\alpha \to \nu_\beta) \simeq P(\bar{\nu}_\alpha \to \bar{\nu}_\beta) \simeq \left| \delta_{\alpha\beta} - \sin^2 2\theta_{\alpha\beta}\ \sin^2\left(\frac{\Delta m^2_{41} L}{4E}\right)\right|,$$

where

$$\sin^2 2\theta_{\alpha\beta} \equiv 4|U_{\alpha 4}|^2 \left|\delta_{\alpha\beta} - |U_{\beta 4}|^2\right| \qquad (\alpha, \beta = e, \mu, \tau, s),$$

so the formula for the oscillation probability reduces to that in the two-flavor framework. In the following subsections, we will discuss the three channels $(\alpha, \beta) = (e, e)$, (μ, e), and (μ, μ). In the parametrization of Eq. (26), we have the following mixing angle:

$$\sin^2 2\theta_{ee} = 4|U_{e4}|^2(1 - |U_{e4}|^2) = \sin^2 2\theta_{14} \tag{27}$$

$$\sin^2 2\theta_{\mu\mu} = 4|U_{\mu 4}|^2(1 - |U_{\mu 4}|^2) = 4c^2_{14}s^2_{24}\left(1 - c^2_{14}s^2_{24}\right) \tag{28}$$

$$\sin^2 2\theta_{\mu e} = 4|U_{\mu 4}|^2|U_{e4}|^2 = s^2_{24}\sin^2 2\theta_{14}. \tag{29}$$

3.1.1 $\nu_e \to \nu_e$ *channel.* To probe neutrino oscillations $\nu_e \to \nu_e$ or $\bar{\nu}_e \to \bar{\nu}_e$ for the region of $0.1\ \mathrm{eV}^2 \lesssim \Delta m^2 \lesssim 10\ \mathrm{eV}^2$, short baseline experiments of electron antineutrinos from reactors or electron neutrinos from radioactive sources have been performed. In 2011 the flux of the reactor neutrino was recalculated in Ref. [53,54] and it was claimed that the normalization is shifted by about +3% on average. If their claim on the reactor neutrino flux is correct, then neutrino oscillation with $\Delta m^2 \gtrsim 1\ \mathrm{eV}^2$ may be concluded from a reanalysis of 19 reactor neutrino results at short baselines [64]. This is called the reactor antineutrino anomaly. The result in 2019 by Daya Bay [65] disfavors the new flux of reactor antineutrinos [54,64] from a shape analysis of the energy spectrum. However, as far as the overall normalization of reactor antineutrinos is concerned, there is uncertainty that is as large as that of the difference between the old and new fluxes [66] and it is not clear whether the reactor antineutrino anomaly is disfavored from the result of Ref. [65]. Among the recent short baseline reactor neutrino experiments, NEOS [67], DANSS [68], STEREO [69], PROSPECT [70], and Neutrino-4 [71], the only experiment that had an affirmative result is Neutrino-4.

On the other hand, it was pointed out in Ref. [55] that the measured and predicted ^{71}Ge production rates differ in the gallium radioactive source experiments GALLEX and SAGE, and this is called the gallium anomaly. The recent affirmative result of the BEST experiment [72] is consistent with the region in $(\sin^2 2\theta_{14},\ \Delta m^2_{41})$, which was suggested by Ref. [55], although most of the BEST region is disfavored by the reactor experiments, except for Neutrino-4.

Figure 5 shows the results of reactor and radioactive source neutrino experiments. There are criticisms on the significance of the affirmative results and readers are referred to Ref. [73] for references. To observe the oscillation pattern at short baseline experiments with low energy, it is necessary to have a detector with very good energy resolution and to have a relatively small reactor core. This is the reason why short baseline experiments become difficult for $\Delta m^2_{41} \gtrsim$ several eV^2. In Ref. [74] it was suggested that we may be able to improve sensitivity to $\sin^2 2\theta_{ee}$ by observing high-energy atmospheric neutrino shower events at a neutrino telescope whose size

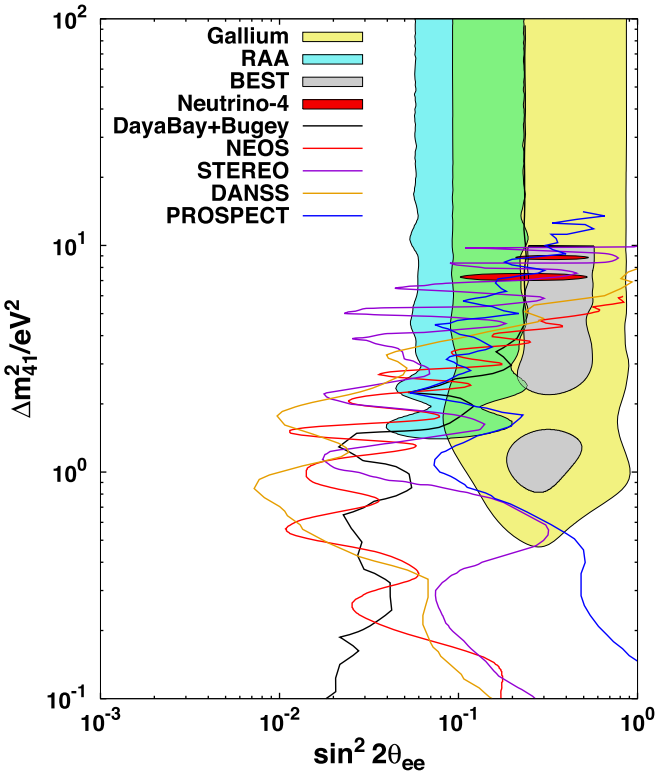

Fig. 5. The excluded and allowed regions for the $\nu_e \to \nu_e$ or $\bar{\nu}_e \to \bar{\nu}_e$ channels. The curves for DayaBay+Bugey (90% CL) [75], NEOS (90% CL) [67], DANSS (90% CL) [68], STEREO (95% CL) [69], and PROSPECT (95% CL) [70] indicate negative results. Those for the gallium anomaly (95% CL) [55], the reactor antineutrino anomaly (RAA) (95% CL) [54,64], Neutrino-4 (90% CL) [71], and BEST (95% CL) [72] are affirmative ones.

is at least 10 times as large as the IceCube facility. The reason why observation of high-energy neutrinos with a very long baseline length is advantageous is because there can be enhancement of the effective mixing angle in matter and therefore the sensitivity can be improved.

3.1.2 $\nu_\mu \to \nu_\mu$ *channel.* Neutrino oscillations $\nu_\mu \to \nu_\mu$ or $\bar{\nu}_\mu \to \bar{\nu}_\mu$ for the region of 0.1 eV^2 $\lesssim \Delta m^2 \lesssim$ 100 eV^2 have been searched by experiments with accelerator (CDHSW [76], CCFR [77], MiniBooNE/SciBooNE [78], and MINOS/MINOS+ [79]) as well as atmospheric (Super-Kamiokande [80] and IceCube [56]) neutrinos. Most of these experiments had negative results, and the only experiment that obtained an affirmative result is IceCube [56], although its significance is weak; i.e., no sterile neutrino hypothesis is disfavored only by $\Delta\chi^2 = 4.94$ for two degrees of freedom, naively corresponding to 1.7σ in the Gaussian distribution.

Figure 6 shows the results of experiments for the disappearance channels of ν_μ or $\bar{\nu}_\mu$.

3.1.3 $\nu_\mu \to \nu_e$ *channel.* Several accelerator-based neutrino experiments have been performed in the past to search for oscillations $\nu_\mu \to \nu_e$ or $\bar{\nu}_\mu \to \bar{\nu}_e$. The only two experiments that reported an affirmative result are LSND [51] and MiniBooNE [52]. Since the early stages of sterile neutrino oscillation study, it has been known [81,82] that the LSND region in the (Δm^2, $\sin^2 2\theta$)-plane has tension with other negative results in the disappearance channels $\nu_e \to \nu_e$ and $\nu_\mu \to \nu_\mu$. By defining $\sin^2 2\theta_{\alpha\beta}$ ($\alpha, \beta = \mu, e$) as a value of the horizontal coordinate as a

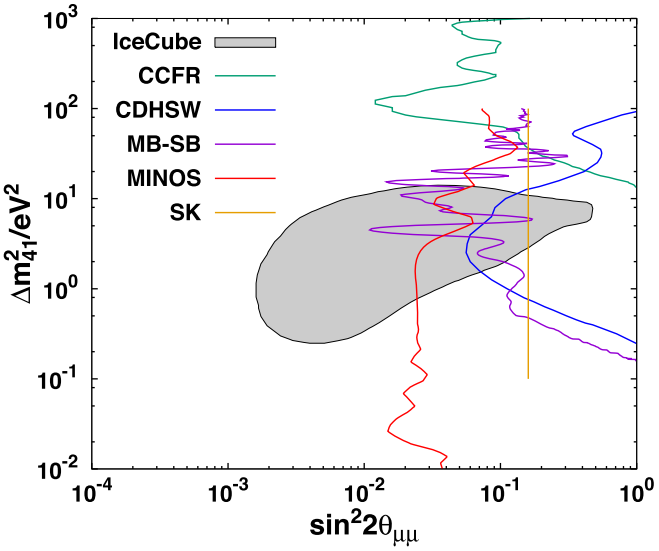

Fig. 6. The excluded and allowed regions for the $\nu_\mu \to \nu_\mu$ or $\bar{\nu}_\mu \to \bar{\nu}_\mu$ channels. The curves for CDHSW (90% CL) [76], CCFR (90% CL) [77], MiniBooNE/SciBooNE (90% CL) [78], Super-Kamiokande (90% CL) [80], and MINOS/MINOS+ (90% CL) [79] indicate negative results. That for IceCube (90% CL) [56] is affirmative.

function of Δm^2_{41} in Figs. 5 and 5, from Eqs. (27) and (28), negative results in the two channels $\nu_e \to \nu_e$ and $\nu_\mu \to \nu_\mu$ at a given value of Δm^2_{41} indicate

$$4|U_{e4}|^2(1-|U_{e4}|^2) < \sin^2 2\theta_{ee}$$
$$4|U_{\mu 4}|^2(1-|U_{\mu 4}|^2) < \sin^2 2\theta_{\mu\mu}. \tag{30}$$

On the other hand, from Eq. (29), an affirmative result in the channel $\nu_\mu \to \nu_e$ leads to

$$4|U_{\mu 4}|^2|U_{e4}|^2 = \sin^2 2\theta_{\mu e}. \tag{31}$$

Assuming $|U_{e4}|^2 \ll 1$, $|U_{\mu 4}|^2 \ll 1$, we have the following inequality at a given value of Δm^2_{41}:

$$\sin^2 2\theta_{\mu e} < \frac{1}{4}\sin^2 2\theta_{ee}\sin^2 2\theta_{\mu\mu}. \tag{32}$$

$\sin^2 2\theta_{ee}$ ($\sin^2 2\theta_{\mu\mu}$) can be regarded as the strongest bound from the negative results of the disappearance channel $\nu_e \to \nu_e$ ($\nu_\mu \to \nu_\mu$). The value of $(1/4)\sin^2 2\theta_{ee}\sin^2 2\theta_{\mu\mu}$ at 90% CL is plotted as a function of Δm^2_{41} in Fig. 7 (indicated as "disappearance(n)") together with the allowed regions suggested by LSND and MiniBooNE, and other negative results. Equation (31) indicates that the allowed region of LSND or MiniBooNE should be the left side of the curve $(1/4)\sin^2 2\theta_{ee}\sin^2 2\theta_{\mu\mu}$ but the MiniBooNE region is on the right side of the "disappearance(n)" curve for all the values of Δm^2_{41} and the LSND region is either on the right side of the "disappearance(n)" curve or it is disfavored by the negative results of other experiments at 90% CL. Thus the results by LSND and MiniBooNE are disfavored by the negative results of other experiments. On the other hand, if we take the affirmative results by Neutrino-4 for $\nu_e \to \nu_e$ and IceCube for $\nu_\mu \to \nu_\mu$ seriously, then the allowed region is the region that is referred to as "disappearance(a)" in Fig. 7. In this case, the mixing $\sin^2 2\theta_{\mu e}$ in the appearance probability $P(\nu_\mu \to \nu_e)$ can be smaller than the present upper bound by more than one order of magnitude for $\Delta m^2_{41} \sim 7$ eV^2 or 9 eV^2, and some part of the "disappearance(a)" region in Fig. 7 is still consistent with all other experiments in the past except LSND and MiniBooNE.

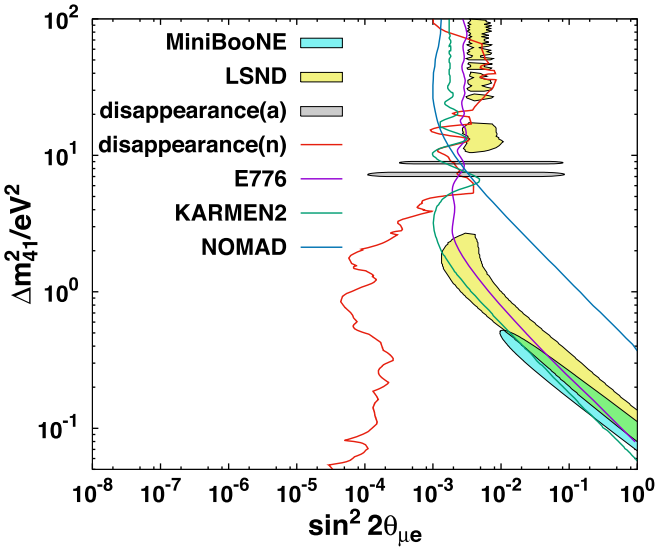

Fig. 7. The excluded and allowed regions for the $\nu_\mu \to \nu_e$ or $\bar{\nu}_\mu \to \bar{\nu}_e$ channels. The curves for E776 (90% CL) [83], KARMEN2 (90% CL) [84], and NOMAD (90% CL) [85] indicate negative results. Those for LSND (90% CL) [51] and MiniBooNE (90% CL) [52] are affirmative ones. "Disappearance(n)" stands for the constraint at 90% CL from the negative results of disappearance channels $\nu_e \to \nu_e$ ($\bar{\nu}_e \to \bar{\nu}_e$) and $\nu_\mu \to \nu_\mu$ ($\bar{\nu}_\mu \to \bar{\nu}_\mu$) as given by Eq. (31). "Disappearance(a)" stands for the possible region at 90% CL that can be inferred if we take seriously the two affirmative results of disappearance channels, i.e., Neutrino-4 ($\bar{\nu}_e \to \bar{\nu}_e$) and IceCube ($\nu_\mu \to \nu_\mu$ and/or $\bar{\nu}_\mu \to \bar{\nu}_\mu$).

The anomalies of LSND, the reactor, and gallium provide the main motivation for studying sterile neutrino oscillations. The search for sterile neutrinos in the same channel $\bar{\nu}_\mu \to \bar{\nu}_e$ as that of LSND is still ongoing [86], and it is hoped that these anomalies will be confirmed in the future.

3.2 *Non-standard interactions in propagation*

If there is a flavor-dependent neutrino non-standard interaction (NSI) in neutrino propagation:

$$\mathcal{L}_{\rm NSI} = -2\sqrt{2}\,\epsilon^{ff'P}_{\alpha\beta} G_F (\overline{\nu}_{\alpha L}\gamma_\mu \nu_{\beta L})(\overline{f}_P \gamma^\mu f'_P), \tag{33}$$

where f_P and f'_P are fermions with chirality P and $\epsilon^{ff'P}_{\alpha\beta}$ is a dimensionless constant normalized in terms of the Fermi coupling constant G_F, then the matter potential in the flavor basis is modified as

$$A \begin{pmatrix} 1+\epsilon_{ee} & \epsilon_{e\mu} & \epsilon_{e\tau} \\ \epsilon_{\mu e} & \epsilon_{\mu\mu} & \epsilon_{\mu\tau} \\ \epsilon_{\tau e} & \epsilon_{\tau\mu} & \epsilon_{\tau\tau} \end{pmatrix}, \tag{34}$$

where $A \equiv \sqrt{2} G_F N_e$ stands for the matter effect, $\epsilon_{\alpha\beta}$ is defined by $\epsilon_{\alpha\beta} \equiv \sum_{f=e,u,d} (N_f/N_e)\epsilon^f_{\alpha\beta}$, and N_f ($f = e, u, d$) stands for number densities of fermions f. Here we define the new NSI parameters as $\epsilon^f_{\alpha\beta} \equiv \epsilon^{ffL}_{\alpha\beta} + \epsilon^{ffR}_{\alpha\beta}$ since the matter effect is sensitive only to coherent scattering and only to the vector part in the interaction.

It was pointed out [57] that there was tension at 2σ between the mass-squared difference from the solar neutrino data ($\Delta m^2_{21} \simeq 4 \times 10^{-5}{\rm eV}^2$) and that of the KamLAND experiment ($\Delta m^2_{21} = 7.5 \times 10^{-5}{\rm eV}^2$). Reference [58] showed that a non-vanishing value of the new NSI parameters $\epsilon^f_{\alpha\beta}$ solves this tension. This fact gives a motivation to take seriously NSI in propagation. The

significance of the anomaly was approximately 2σ in 2016 [57], but it had reduced to 1.4σ in 2020 [30]. If the significance keeps decreasing in the future, then this should not be listed in the list of anomalies.

4. Impact of Professor Koshiba on neutrino physics

Today we have a lot of information on neutrinos, such as the two mass-squared differences, three mixing angles, and a hint of a CP-violating phase. In the process of gaining such information, Professor Masatoshi Koshiba made outstanding contributions to the field, by the Kamiokande experiment, which was proposed by him in 1979 [87] and was started in 1983, and by the Super-Kamiokande experiment, which was again proposed by him in 1983 [88][1] and was started in 1996. The significant feature of the Kamiokande and Super-Kamiokande experiments is that they give information on the energy spectrum and the zenith angle dependence of neutrinos, which plays a crucial role in discovering neutrino oscillations. He even proposed an idea of a megaton-class water Cherenkov detector in 1992 [90][2], and this is now being turned into reality as the Hyper-Kamiokande experiment [48]. Now it is evident that huge numbers of neutrino events are required to determine the leptonic CP phase, and a megaton-class water Cherenkov detector is ideal for that purpose.

In the standard framework of three massive neutrinos, the remaining quantities to be measured are the sign of Δm^2_{31}, the sign of $\theta_{23} - 45^\circ$, and the CP phase δ. These quantities are expected to be determined by the huge underground neutrino experiments in the near future. On the other hand, to complete the picture of the Standard Model with three massive neutrinos, we need to exclude the anomalies mentioned in Section 3. If we cannot exclude or confirm them by experiments in the near future, then we may need a new type of experiment, which even Professor Koshiba could not imagine.

Acknowledgements

When I was an undergraduate student, I had an opportunity to participate in an experiment under Prof. Koshiba's guidance. Some 20 years later, when we organized NuFact04 Summer Institute at Tokyo Metropolitan University, Prof. Koshiba kindly accepted our invitation to give a talk [91] for students and postdocs, who were strongly impressed by his presentation. I would like to thank Prof. Koshiba for many things; for his guidance during my undergraduate studies, for giving a wonderful talk at NuFact04 Summer Institute, and, among others, for his great contributions to neutrino physics. This research was partly supported by a Grant-in-Aid for Scientific Research of the Ministry of Education, Science and Culture, under Grants No. 18K03653, No. 18H05543, and No. 21K03578.

Funding

Open Access funding: SCOAP[3].

[1] It was initially named JACK (Japan–America Collaboration at Kamioka), and was named Super-Kamiokande in 1984 [89].

[2] It was named DOUGHNUTS (Detector of Under-Ground Hideous Neutrinos from Universe and from Terrestrial Sources) in Ref. [90].

References

[1] Y. Fukuda et al. [Super-Kamiokande Collaboration], Phys. Rev. Lett. **81**, 1562 (1998) [arXiv:hep-ex/9807003] [Search INSPIRE].
[2] B. Pontecorvo, Sov. Phys. JETP **6**, 429 (1957) [Zh. Eksp. Teor. Fiz. **33**, 549 (1957)] [Search INSPIRE].
[3] Z. Maki, M. Nakagawa, and S. Sakata, Prog. Theor. Phys. **28**, 870 (1962).
[4] L. Wolfenstein, Phys. Rev. D **17**, 2369 (1978).
[5] S. P. Mikheyev and A. Y. Smirnov, Sov. J. Nucl. Phys. **42**, 913 (1985) [Search INSPIRE].
[6] M. Apollonio et al. [CHOOZ Collaboration], Phys. Lett. B **466**, 415 (1999) [arXiv:hep-ex/9907037] [Search INSPIRE].
[7] K. Eguchi et al. [KamLAND Collaboration], Phys. Rev. Lett. **90**, 021802 (2003) [arXiv:hep-ex/0212021] [Search INSPIRE].
[8] J. Hosaka et al. [Super-Kamiokande Collaboration], Phys. Rev. D **73**, 112001 (2006) [arXiv:hep-ex/0508053] [Search INSPIRE].
[9] A. Cervera, A. Donini, M. B. Gavela, J. J. Gomez Cadenas, P. Hernandez, O. Mena, and S. Rigolin, Nucl. Phys. B **579**, 17 (2000); 593, 731 (2001) [erratum] [arXiv:hep-ph/0002108] [Search INSPIRE].
[10] V. Barger, D. Marfatia, and K. Whisnant, Phys. Rev. D **65**, 073023 (2002) [arXiv:hep-ph/0112119] [Search INSPIRE].
[11] O. Yasuda, New J. Phys. **6**, 83 (2004) [arXiv:hep-ph/0405005] [Search INSPIRE].
[12] J. Burguet-Castell, M. B. Gavela, J. J. Gomez-Cadenas, P. Hernandez, and O. Mena, Nucl. Phys. B **608**, 301 (2001) [arXiv:hep-ph/0103258] [Search INSPIRE].
[13] H. Minakata and H. Nunokawa, J. High Energy Phys. **0110**, 001 (2001) [arXiv:hep-ph/0108085] [Search INSPIRE].
[14] G. L. Fogli and E. Lisi, Phys. Rev. D **54**, 3667 (1996) [arXiv:hep-ph/9604415] [Search INSPIRE].
[15] K. Abe et al. [T2K Collaboration], Phys. Rev. Lett. **107**, 041801 (2011) [arXiv:1106.2822 [hep-ex]] [Search INSPIRE].
[16] P. Adamson et al. [MINOS Collaboration], Phys. Rev. Lett. **107**, 181802 (2011) [arXiv:1108.0015 [hep-ex]] [Search INSPIRE].
[17] Y. Abe et al. [Double Chooz Collaboration], Phys. Rev. Lett. **108**, 131801 (2012) [arXiv:1112.6353 [hep-ex]] [Search INSPIRE].
[18] F. P. An et al. [Daya Bay Collaboration], Phys. Rev. Lett. **108**, 171803 (2012) [arXiv:1203.1669 [hep-ex]] [Search INSPIRE].
[19] J. K. Ahn et al. [RENO Collaboration], Phys. Rev. Lett. **108**, 191802 (2012) [arXiv:1204.0626 [hep-ex]] [Search INSPIRE].
[20] K. Abe et al. [T2K Collaboration], Phys. Rev. D **103**, 112008 (2021) [arXiv:2101.03779 [hep-ex]] [Search INSPIRE].
[21] M. A. Acero et al. [NOvA Collaboration], arXiv:2108.08219 [hep-ex] [Search INSPIRE].
[22] M. C. Gonzalez-Garcia, M. Maltoni, and T. Schwetz, Universe **7**, 459 (2021) [arXiv:2111.03086 [hep-ph]] [Search INSPIRE].
[23] F. Capozzi, E. Di Valentino, E. Lisi, A. Marrone, A. Melchiorri, and A. Palazzo, Phys. Rev. D **104**, 083031 (2021) [arXiv:2107.00532 [hep-ph]] [Search INSPIRE].
[24] P. F. de Salas, D. V. Forero, S. Gariazzo, P. Martínez-Miravé, O. Mena, C. A. Ternes, M. Tórtola, and J. W. F. Valle, J. High Energy Phys. **2102**, 071 (2021) [arXiv:2006.11237 [hep-ph]] [Search INSPIRE].
[25] B. T. Cleveland, T. Daily, R. Davis, Jr., J. R. Distel, K. Lande, C. K. Lee, P. S. Wildenhain, and J. Ullman, Astrophys. J. **496**, 505 (1998).
[26] F. Kaether, W. Hampel, G. Heusser, J. Kiko, and T. Kirsten, Phys. Lett. B **685**, 47 (2010) [arXiv:1001.2731 [hep-ex]] [Search INSPIRE].
[27] J. N. Abdurashitov et al. [SAGE Collaboration], Phys. Rev. C **80**, 015807 (2009) [arXiv:0901.2200 [nucl-ex]] [Search INSPIRE].
[28] J. P. Cravens et al. [Super-Kamiokande Collaboration], Phys. Rev. D **78**, 032002 (2008) [arXiv:0803.4312 [hep-ex]][Search INSPIRE].
[29] K. Abe et al. [Super-Kamiokande Collaboration], Phys. Rev. D **83**, 052010 (2011) [arXiv:1010.0118 [hep-ex]] [Search INSPIRE].
[30] Y. Nakajima, Proc. XXIX Int. Conf. Neutrino Physics and Astrophysics (2020),.

[31] B. Aharmim et al. [SNO Collaboration], Phys. Rev. C **88**, 025501 (2013) [arXiv:1109.0763 [nucl-ex]] [Search INSPIRE].
[32] G. Bellini et al., Phys. Rev. Lett. **107**, 141302 (2011) [arXiv:1104.1816 [hep-ex]] [Search INSPIRE].
[33] G. Bellini et al. [Borexino Collaboration], Phys. Rev. D **82**, 033006 (2010) [arXiv:0808.2868 [astro-ph]] [Search INSPIRE].
[34] G. Bellini et al. [Borexino Collaboration], Nature **512**, 383 (2014).
[35] A. Gando et al. [KamLAND Collaboration], Phys. Rev. D **88**, 033001 (2013) [arXiv:1303.4667 [hep-ex]] [Search INSPIRE].
[36] K. Abe et al. [Super-Kamiokande Collaboration], Phys. Rev. D **97**, 072001 (2018) [arXiv:1710.09126 [hep-ex]] [Search INSPIRE].
[37] M. G. Aartsen et al. [IceCube Collaboration], Phys. Rev. D **91**, 072004 (2015) [arXiv:1410.7227 [hep-ex]] [Search INSPIRE].
[38] J. P. Yanez et al. [IceCube Collaboration], IceCube oscillations: 3 years muon neutrino disappearance data (available at: http://icecube.wisc.edu/science/data/nu_osc).
[39] T. Bezerra, Proc. XXIX Int. Conf. Neutrino Physics and Astrophysics (2020)..
[40] D. Adey et al. [Daya Bay Collaboration], Phys. Rev. Lett. **121**, 241805 (2018) [arXiv:1809.02261 [hep-ex]] [Search INSPIRE].
[41] J. Yoo, Proc. XXIX Int. Conf. Neutrino Physics and Astrophysics (2020)..
[42] P. Adamson et al. [MINOS Collaboration], Phys. Rev. Lett. **110**, 251801 (2013) [arXiv:1304.6335 [hep-ex]] [Search INSPIRE].
[43] P. Dunne, Proc. XXIX Int. Conf. Neutrino Physics and Astrophysics (2020)..
[44] A. Himmel, Proc. XXIX Int. Conf. Neutrino Physics and Astrophysics (2020)..
[45] P. Adamson et al. [MINOS Collaboration], Phys. Rev. Lett. **110**, 171801 (2013) [arXiv:1301.4581 [hep-ex]] [Search INSPIRE].
[46] K. Abe et al. [Hyper-Kamiokande Proto-Collaboration], Prog. Theor. Exp. Phys. **2015**, 053C02 (2015) [arXiv:1502.05199 [hep-ex]] [Search INSPIRE].
[47] R. Acciarri et al. [DUNE Collaboration], arXiv:1512.06148 [physics.ins-det] [Search INSPIRE].
[48] K. Abe et al., arXiv:1109.3262 [hep-ex] [Search INSPIRE].
[49] S. Fukasawa, M. Ghosh, and O. Yasuda, Nucl. Phys. B **918**, 337 (2017) [arXiv:1607.03758 [hep-ph]] [Search INSPIRE].
[50] K. N. Abazajian et al., arXiv:1204.5379 [hep-ph] [Search INSPIRE].
[51] A. Aguilar et al. [LSND Collaboration], Phys. Rev. D **64**, 112007 (2001) [arXiv:hep-ex/0104049] [Search INSPIRE].
[52] A. A. Aguilar-Arevalo et al. [MiniBooNE Collaboration], Phys. Rev. D **103**, 052002 (2021) [arXiv:2006.16883 [hep-ex]] [Search INSPIRE].
[53] T. A. Mueller et al., Phys. Rev. C **83**, 054615 (2011) [arXiv:1101.2663 [hep-ex]] [Search INSPIRE].
[54] P. Huber, Phys. Rev. C **84**, 024617 (2011); 85, 029901 (2012) [erratum] [arXiv:1106.0687 [hep-ph]] [Search INSPIRE].
[55] C. Giunti and M. Laveder, Phys. Rev. D **77**, 093002 (2008) [arXiv:0707.4593 [hep-ph]] [Search INSPIRE].
[56] M. G. Aartsen et al. [IceCube Collaboration], Phys. Rev. Lett. **125**, 141801 (2020) [arXiv:2005.12942 [hep-ex]] [Search INSPIRE].
[57] K. Abe et al. [Super-Kamiokande Collaboration], Phys. Rev. D **94**, 052010 (2016) [arXiv:1606.07538 [hep-ex]] [Search INSPIRE].
[58] M. C. Gonzalez-Garcia and M. Maltoni, J. High Energy Phys. **1309**, 152 (2013) [arXiv:1307.3092 [hep-ph]] [Search INSPIRE].
[59] M. Maltoni and A. Y. Smirnov, Eur. Phys. J. A **52**, 87 (2016) [arXiv:1507.05287 [hep-ph]] [Search INSPIRE].
[60] M. M. Guzzo, A. Masiero, and S. T. Petcov, Phys. Lett. B **260**, 154 (1991).
[61] E. Roulet, Phys. Rev. D **44**, 935 (1991).
[62] P. A. Zyla et al. [Particle Data Group], Prog. Theor. Exp. Phys. **2020**, 083C01 (2020).
[63] M. Maltoni, T. Schwetz, M. A. Tortola, and J. W. F. Valle, New J. Phys. **6**, 122 (2004) [arXiv:hep-ph/0405172] [Search INSPIRE].
[64] G. Mention, M. Fechner, T. Lasserre, T. A. Mueller, D. Lhuillier, M. Cribier, and A. Letourneau, Phys. Rev. D **83**, 073006 (2011) [arXiv:1101.2755 [hep-ex]] [Search INSPIRE].

[65] D. Adey et al. [Daya Bay Collaboration], Phys. Rev. Lett. **123**, 111801 (2019) [arXiv:1904.07812 [hep-ex]] [Search INSPIRE].
[66] A. C. Hayes, J. L. Friar, G. T. Garvey, G. Jungman, and G. Jonkmans, Phys. Rev. Lett. **112**, 202501 (2014) [arXiv:1309.4146 [nucl-th]] [Search INSPIRE].
[67] Y. J. Ko et al. [NEOS Collaboration], Phys. Rev. Lett. **118**, 121802 (2017) [arXiv:1610.05134 [hep-ex]] [Search INSPIRE].
[68] I. Alekseev et al. [DANSS Collaboration], Phys. Lett. B **787**, 56 (2018) [arXiv:1804.04046 [hep-ex]] [Search INSPIRE].
[69] H. Almazán et al. [STEREO Collaboration], Phys. Rev. D **102**, 052002 (2020) [arXiv:1912.06582 [hep-ex]] [Search INSPIRE].
[70] M. Andriamirado et al. [PROSPECT Collaboration], Phys. Rev. D **103**, 032001 (2021) [arXiv:2006.11210 [hep-ex]] [Search INSPIRE].
[71] A. P. Serebrov et al.,Phys. Rev. D **104**, 032003 (2021) [arXiv:2005.05301 [hep-ex]] [Search INSPIRE].
[72] V. V. Barinov et al., arXiv:2109.11482 [nucl-ex] [Search INSPIRE].
[73] M. S. Athar et al., , Prog. Part. Nucl. Phys. **124**, 103947 (2022) [arXiv:2111.07586] [hep-ph][Search INSPIRE].
[74] Y. Wang and O. Yasuda, Prog. Theor. Exp. Phys. **2022**, 023B04 (2022)[arXiv:2110.12655] [hep-ph][Search INSPIRE].
[75] P. Adamson et al. [Daya Bay MINOS Collaborations], Phys. Rev. Lett. **117**, 151801 (2016) [arXiv:1607.01177 [hep-ex]] [Search INSPIRE].
[76] F. Dydak et al., Phys. Lett. B **134**, 281 (1984).
[77] I. E. Stockdale et al., Phys. Rev. Lett. **52**, 1384 (1984).
[78] K. B. M. Mahn et al. [SciBooNE and MiniBooNE Collaborations], Phys. Rev. D **85**, 032007 (2012) [arXiv:1106.5685 [hep-ex]] [Search INSPIRE].
[79] P. Adamson et al. [MINOS+ and Daya Bay Collaborations], Phys. Rev. Lett. **125**, 071801 (2020) [arXiv:2002.00301 [hep-ex]] [Search INSPIRE].
[80] K. Abe et al. [Super-Kamiokande Collaboration], Phys. Rev. D **91**, 052019 (2015) [arXiv:1410.2008 [hep-ex]] [Search INSPIRE].
[81] N. Okada and O. Yasuda, Int. J. Mod. Phys. A **12**, 3669 (1997) [arXiv:hep-ph/9606411] [Search INSPIRE].
[82] S. M. Bilenky, C. Giunti, and W. Grimus, Eur. Phys. J. C **1**, 247 (1998) [arXiv:hep-ph/9607372] [Search INSPIRE].
[83] L. Borodovsky et al., Phys. Rev. Lett. **68**, 274 (1992).
[84] B. Armbruster et al. [KARMEN Collaboration], Phys. Rev. D **65**, 112001 (2002) [arXiv:hep-ex/0203021] [Search INSPIRE].
[85] P. Astier et al. [NOMAD Collaboration], Phys. Lett. B **570**, 19 (2003) [arXiv:hep-ex/0306037] [Search INSPIRE].
[86] M. Harada et al. [JSNS2 Collaboration], arXiv:1310.1437 [physics.ins-det] [Search INSPIRE].
[87] Y. Watanabe, Proc. Workshop Unified Theories and the Baryon Number in the Universe, KEK Report 79-18, 53 (1979) [Search INSPIRE].
[88] M. Koshiba [Kamiokande Collaboration], Proc. Workshop Grand Unified Theories and Cosmology, KEK Report 84-12, 24 (1983) (available at: https://lss.fnal.gov/conf/C831207.1/kek-84-12.pdf).
[89] M. Koshiba, Proc. 22nd Int. Conf. High-Energy Physics, Vol. **2**, p. 67 (1984) (available at: https://inspirehep.net/files/bb83a8492ad3b39b99fe1cc7fc26e030).
[90] M. Koshiba, Phys. Rept. **220**, 229 (1992).
[91] M. Koshiba, Talk at 3rd International School on Neutrino Factories and Superbeams (2004) (available at: http://musashi.phys.se.tmu.ac.jp/NuFact04_SI/lectures/koshiba-e.pdf).